SCIENTIA
AGRICULTURAE
BOHEMICA

Article

Understanding Effects of Ag and Fe_3O_4 Nanoparticles in Morpho-biochemical Variations of Seeds and its Localization

Shatabdi Basu[1], Nidhi Sahu[1], Madhubala Kumari[1] and Koel Mukherjee[1]*

[1] Department of Bioengineering and Biotechnology, Birla Institute of Technology, Mesra, Ranchi Jharkhand 835215 India; shabwarrock@gmail.com; nidhi.125sahu@gmail.com; kmadhubala121@gmail.com; koelmukherjee@bitmesra.ac.in

* Correspondence: koelmukherjee@bitmesra.ac.in (India)

Abstract: The primary focus of the current work was to synthesis Ag and Fe_3O_4 NPs through chemical routes and their varied concentration effect in the germination-seedling growth of *Macrotyloma uniflorum* (Kulthi bean) and *Lens culinaris* (Masoor) seeds, respectively. The synthesized nanoparticles were characterized by various physiochemical techniques (UV-Vis, DLS, FTIR, and FESEM). Four different concentrations of Ag and Fe_3O_4 NPs were applied on *Lens culinaris* and *Macrotyloma uniflorum* and positive influence was noticed for shoot-root length, chlorophyll, protein and starch content. Statistical analysis for every treatment was done with 3 replicates and results were analysed by one-way ANOVA using Minitab Version 16. Further, for getting information on the accumulation of nanoparticles in particular regions of plant body, ICP-OES study was also performed. The distinctive crystals of a black red colour in plant tissue was possible to identify the NPs localization in several seedling segments. Chemically synthesized metal-based nanoparticles have shown better effect on seed germination and have less hazardous impacts on the surrounding environment which make them a better alternative for commercially available agrochemicals.

Keywords: Nanoparticles; *Lens culinaris; Macrotyloma uniflorum*; NPs localization

Received for publication on 15.12.2023

Accepted for publication on 20.01.2025

1. Introduction

Nanotechnology is a very rapid developing subject and has huge applications in the field of agriculture (Singh et al., 2021). Nanotechnology can increase the potential of crop yield and it can

boost the production in the field, encourage sustainable practises, and guarantee food security (Rastogi et al., 2017). The effects of nanoparticles (NPs) on plants depend on many factors such as types of NPs, its concentration and size, as well as the plant species and its stage of development. It has been discovered that nanoparticles can alter a variety of physiological indices in plants, including the germination rate, number of leaves, root elongation, and biomass. The recurring inquisitiveness about Ag and Fe_3O_4NPs in the nanotechnology and agriculture field has shown optimum effectiveness over the last few years (Seleiman et al., 2020). It enhances seed germination and plant growth and improves the photosynthesis route. They play a vital role in food security and improving crop production (Kumari et al., 2023). Additionally, they play a vital role in agriculture by having several applications that are crucial for ensuring food security and improving crop production (Kashyap et al., 2023; Mehmood et al., 2018). Moreover, they also function as pesticides, supplying adequate doses to the target parts of the crops without emitting extreme pesticides into the environment (Khan et al., 2023).

Seed germination is a significant phenomenon in modern agriculture, because it is a lifeline for plants that ensures their survival. Due to this astounding growth in the application of nanotechnology in agriculture, it is alluring to comprehend the nature in which silver nanoparticles (Ag NPs) and iron oxide (Fe_3O_4 NPs) affect seed germination (Iravani et al., 2014). A great attention can be seen currently drawn in nanoparticles in plants for their much-hyped potential to enhance crop yield. Recently, practices using silver (Ag) and iron oxide (FeO) nanoparticles are gaining more acceptances to contribute innovative solutions in various applications such as agriculture. Lens culinaris is a little, tall, delicately pubescent plant which is sometimes referred to as Adas, lentils, or Masoor (Priester et al., 2012). It is typically grown as a significant diet crop in temperate western Asia, south-eastern Europe, and North India. The lenticular, smooth, and compressed seeds are a good source of vitamin B, calcium, iron, and other vital elements. They are a significant dietary source in many nations, consumed as whole grains, and have large protein, carbohydrate, and fibre contents (Ma et al., 2015). Alpha galactosides, non-reducing sucrose derivatives, raffinose (trisaccharide), stachyose (tetrasaccharide), and verbascose (pentasaccharide) are all found in large quantities in lentil seeds (Rizwan et al., 2017). Previous studies have shown that nanoparticles can boost plant growth and promote plant growth by regulating the growth and function of commensal microbes. It was also briefed that these nanoparticles promoted plant health through improved root nodulation effect (Rui et al., 2016). Horse gramme (local name kulth and kulthi-kalai) is a good source of antioxidants, minerals, and vitamins at a reasonable price (Yang et al., 2017). It has 18.5-28.5% protein, 50–70% carbs, 6.26% fat, 7.46% fibre, 0.31% phosphorus, 0.93% iron, 5.31% ash, and 0.28% calcium. Horse gramme seeds are favoured for decreasing cholesterol, preventing skin rashes, and preventing kidney stones. Additionally, those with rheumatism, cough, oedema, bronchitis, jaundice, and hyperglycemia should prefer to consume it. (Arora et al., 2022).

The use of nanoparticles in plant systems has attracted a lot of attention for their potential to boost crop yield promote plant well-being and tackle challenges. Silver (Ag) and iron oxide (FeO) nanoparticles have shown promise in practices (Kaningini et al., 2022). Silver nanoparticles (Ag NPs) have the ability to hinder the attack from different microorganisms and varied range of pathogens. This is a very important property of silver nanoparticles as it helps in boosting stronger plant growth and also in reducing plant diseases due to its antimicrobial property (Mahawar et al., 2018). Different studies and literature have helped us to know that it is very effective in controlling

Fusarium, a pathogen, bacterial diseases and also boosting resistance against pathogens like *Pseudomonas syringae* (Chen et al., 2015). Ag NPs can stimulate plant growth by regulating phytohormone levels enhancing absorption and encouraging root development. It is very crucial in improving the crop health (Rico et al., 2014; Brindaban et al., 2015). Furthermore, examples research has shown that silver nanoparticles (Ag NPs) have the ability to stimulate the synthesis of gibberellins, a kind of plant hormones that encourage stem advancement and seed germination. This chemical shift can result in growing vitality and more production in agriculture Research conducted with crops such as corn and rice have showed that Ag NPs, which can considerably alter the anatomy of roots resulting in transpiration and absorbance of nutrients (Chen et al., 2011).

Iron oxide nanoparticles FeO NPs are frequently utilised as micronutrient fertilisers. Their large area of surface compared to volume ratio, which permits a larger intake from the roots of plants, making their nanoscale dimension advantageous. Through increasing the rate of photosynthesis while improving intake of nutrients, especially of phosphorus, iron, and various other elements, these promotors help plants develop rapidly. Additionally, they assist in the adjustment of plants to stress-related genetic modifications allowing them to withstand undesirable conditions in the environment (Alidoust et al., 2013). Inoculation of iron oxide nanoparticles can restore soil fertility and has potential to assist in the remediation contaminated soils (Seleiman et al., 2020). Their controlled release mechanisms help to deliver nutrients in synchronization with plant demands, which minimizes the risk of nutrient leaching and increases overall soil fertility. Moreover, FeO NPs have been demonstrated to increase the activity of iron enzymes such as peroxidase and catalase, which're essential for plant handling stress as well as metabolic processes (Avila-Quezada et al., 2022).

Even though there are many advantages of using silver and iron oxide nanoparticles, there are a few things that need to be considered. The effect of these nanoparticles in the food chain and their toxicity to target organisms in long terms are a few things that needs to be studied further in upcoming years and research should be done in these areas. Their effect in food chain after long terms and their side effects are yet to be studied. Besides, there is still much to learn about how nanoparticles interact with plant systems, necessitating investigation into their mechanisms of action and long-term consequences. For example, the processes involved in the absorption, translocation and metabolism of Ag NPs and FeO NPs within plants are not fully understood. Gaining insight into these mechanisms is vital, for optimizing nanoparticle formulations and application techniques to maximize benefits while minimizing risks. In this research we thoroughly examine the existing body of work on using silver and iron oxide nanoparticles in plants with a focus, on how they affect plant growth well-being and output. We also discuss the pros and cons of their usage providing hints at prospective research areas where future researchers can work on. We are also saying that based on the data we have worked upon, it looks like Ag NPs (silver nanoparticles) and FeO NPs (iron oxide nanoparticles), contribute towards modern agriculture (Chen et al., 2011). This kind of analysis lays the groundwork for research that might sculpt an effective nanoparticle-based strategy to improve crop yield and food security. Recent studies showed that plant response to Ag NPs is associated with their dosage, which can either enhance or inhibit growth. Exposure to specific and serial Ag NPs enhances plant growth more than control plants, whereas low and high concentrations negatively affect plant growth. Several reports suggest

that proper concentrations of Ag NPs are vital in enhancing plant growth/seed germination, improving chlorophyll content/photosynthetic efficiency, and increasing fertilizer (Khan et al., 2021).

Both the nanoparticles play major role to improve soil quality by removing soil contaminants enhance the nutrients and water availability to plant roots and also increase the crop productivity. The projected paper intends to study the morpho-biochemical changes in two different seeds (*L. culinaris* and *M. uniflorum*) after treating with chemically synthesized Ag and Fe_3O_4 NPs. Various parameters such as germination percentage, chlorophyll content, protein and starch content of the seedlings were performed in this paper. Further to study the localization of these two nanoparticles ICP-OES study was conducted. On future aspect further it can be studied that how these nanoparticles could go at par with eco-friendly methods of farming for a long-term process without showing any other consequences.

2. Materials and Methods

2.1 Chemical synthesis of silver (Ag) and iron oxide (Fe_3O_4) NPs

Silver nitrate ($AgNO_3$), Sodium borohydrate ($NaBH_4$) and sodium dodecyl sulfate (SDS) was used as the precursor, reducing agent and stabilizer respectively for the synthesis of silver nanoparticles (Ag NPs) using reduction method (Hao et al., 2016). However, the co-precipitation method was applied to synthesize Fe_3O_4 NPs where ferric chloride hexahydrate ($FeCl_3.6H_2O$) and ferrous sulphate heptahydrate ($FeSO_4.7H_2O$) were used as the precursor.

2.2 Characterization of synthesized nanoparticles

Preliminary characterization of the Ag and Fe_3O_4 NPs was carried out using UV-Visible spectroscopy. UV-Visible absorption measurements were carried out at room temperature on Analytical Dual Beam UV-VIS 3100XE Spectrophotometer using a quartz cell with 1cm path length. The spectra of Ag and Fe_3O_4 NPs solution was monitored by UV-Vis spectrophotometer from 200-450nm (Noori et al., 2020). For DLS, the sample was oven dried at 55°C overnight and tested in Zetasizer Nano ZS, Malvern Instruments Ltd., UK, The FTIR spectrum of chemically synthesizes Ag and Fe_3O_4 nanoparticles was recorded on a FTIR instrument PerkinElmer Frontier FTIR Spectrometer at a resolution of $4cm^{-1}$ attachment in the range of $400\text{-}4000cm^{-1}$(Bombin et al., 2015). FESEM (MIRA3 TESCAN) was used to observe the surface morphology of the samples with an operating voltage of 10 kV. All the measurement was carried out in duplicate.

2.3 Experimental setup

Four concentrations (10 µg/ml, 20 µg/ml, 30 µg/ml, 40 µg/ml) of each type of nanoparticles were selected for the study (Doolette et al., 2015). 25 seeds of each plant (*Lens culinaris* and *Macrotyloma uniflorum*) were taken in petriplates. Seeds were immersed in a 0.1% mercuric chloride solution for 5 min for surface sterilization and then these seeds were added with 30 ml of the solution in each petriplates. The experiments were performed in triplicates. The seeds were left for 7-10 days for germination.

2.4 Morpho-biochemical studies

2.4.1 Germination rate/Percentage

After 7 days only some of the seeds started germinating and rate was calculated to find the positive or negative effect of nanoparticles on plant growth. The formula used for calculating germination percentage is as follows:

Germination Percentage = seeds germinated/total seeds x 100.

2.4.2 Root and shoot length

Root lengths of each germinated seeds were taken by cm scale and forceps. Tip to tip measurements were done and average was calculated. Similarly, shoot lengths of each germinated seeds were taken using tip to tip measurements and average was performed.

2.4.3 Statistical analysis

Statistical analysis for every treatment was done with triplicates and error bar were plotted against mean with standard deviation. Additionally, results were analysed by one-way ANOVA with used Minitab Version 16 (Tavares et al., 2012).

2.4.4 Chlorophyll estimation procedure

1gm of leaf sample was weighed and chopped in mortar pestle. 20ml of 80% acetone and 0.5 gm of $MgCO_3$ was added and properly grinded. Then the paste was transferred in centrifuge tube and kept in refrigerate for 4 hours (Rashid et al., 2013). After refrigeration, centrifugation was performed for 500rpm for 5 min. Supernatant was collected in 100ml flask and further the volume was maintained up to 200ml using 80% acetone. Absorbance readings were performed at wavelengths of 663 nm and 645 nm. The obtained values were substituted in the following formulas, described in, for the estimation of photosynthetic pigments.

- Chlorophyll a (mg/g) = (12.7 * A663) − (2.69 * A645)
- Chlorophyll b (mg/g) = (22.9 * A645) − (4.68 * A663)
- Chlorophyll total (mg/g) = (8.2 * A663) + (20.2 * A645)

Where, A663 and A645 are the absorbance measured from 663 nm and 645 nm, respectively.

2.4.5 Protein estimation by Lowry method

For protein estimation stock solution was prepared by dissolving 100mg of BSA in 100ml distilled water making the final concentration of stock solution - 1mg/ml. Standard graph was prepared by plotting concentration of the standard BSA in X- axis and absorbance in Y- axis. 2 gm of sample was weighed and added to 9ml of distilled water and was finely grounded in mortar pestle in presence of ice box to avoid protein degradation. The sample was then centrifuged at 4°C at 10000rpm for 10mins. Out of 20 test tubes, the 1st one was served as blank. After 10 min incubation, 0.5ml of Folin Ciocalteu was added to each and it was left for 30 minutes incubation (Elamawi et al., 2018).

Further, it was kept in incubation in the dark at room temperature for 30 min. After incubation OD was taken in UV-Vis spectrophotometer at 660nm against the blank.

2.4.6 Starch estimation

Standard curve of D- glucose for reducing sugar was arranged by preparing of stock solution where 100mg of glucose was dissolving in 100ml distilled water making the final concentration of stock solution is 1mg/ml (Song et al., 2009). Standard graph was prepared by plotting concentration of the standard Glucose in X- axis and absorbance in Y- axis. After standard curve plotted,2 gm of sample was weighed, smashed and boiled after adding 20ml of ethanol. After 30 mins the full contain was stained and kept open for ethanol evaporation. Further, 100ml of water was added to each test tube and allowed to mixed (Chaki et al., 2015). 1sttest tube is taken as blank with distilled water in place of sample. 4ml of Anthrone's reagent was added in rest of the test tubes. The absorbance was taken in UV-Vis spectrophotometer at 540nm against the blank.

2.5 Localization study of Ag NPs and Fe_3O_4 NPs

The 3 weeks seedlings were macerated by submerging them in 10% NaOH for 48 hours, and then the excess NaOH was rinsed away with distilled water. To study under a compound microscope (40x), the segmented root and stem (1 cm in length) were placed on a glass slide, covered with a cover slip, and lightly tapped to disperse the tissue even after stained with safranin (Chaki et al., 2015). For deeper study, ICP-OES was performed after 8 days of addition of nanoparticles to the seeds. Test was performed using Optical 21000V ICP-OES available in Central Instrumentation Facility of BIT Mesra.

3. RESULTS AND DISCUSSION

Ag NPs was synthesized by chemical reduction method and the colour of the solution turned dark yellow which indicated the formation of Ag NPs (Jemal et al., 2017). Similarly, Fe_3O_4 NPs was synthesized by co-precipitation method and colour of the solution turned black which indicated the formation of Fe_3O_4 NPs in a precipitate form (Kiwumulo et al., 2022).

3.1 Characterization

The synthesis of the Ag NPs in aqueous solution was analysed by recording the absorption spectra at a wavelength range of 300-450 nm (Fig. 1A). From the absorption spectra it was observed that the broad surface plasmon resonance (SPR) peak was at 400nm that confirmed the synthesis of Ag NPs. From the past studies, it was reported that SPR peak located at 400 and 450nm indicates the presence of Ag NPs (Jemal et al., 2017).

The synthesis of the Fe_3O_4 NPs in aqueous solution was analysed by recording the absorption spectra. Result (Fig. 1B) indicates no prominent peak but previously is reported that (Kiwumulo et al., 2022) that wavelength range of 200-300nm indicates the presence of Fe_3O_4 NPs. From the absorption spectra it was observed that the surface plasmon resonance (SPR) peak was observed at 206nm, while the absorption edge lies between 200-270nm. Dynamic light scattering is mainly used

to determine the nanoparticles size, but also evaluate their stability over time in suspension, at different pH and temperature condition (Zaheer et al., 2012). The measurement gave the average size of the nanoparticles, the peak value and the polydispersity index (PdI) that describes the width of the particle size distribution. The PdI scale ranges from 0 to 1 (0 is for monodisperse and 1 is for polydisperse). The data of DLS showed that the Z-average (nm) was 44 nm and 0.468 PdI value. The three peaks indicated the quality of the synthesized Ag NPs (Fig. 1A). It also indicated that the variable sizes of Ag NPs were found in the solution. The value of zeta potential of the Ag NPs was -22.3 mV. The data of DLS showed that the Z-average (nm) was 99 nm and 0.579 PdI value (Fig. 1B) for Fe_3O_4 NPs. FTIR spectra analysis were carried out to identify the various types of functional group present in the biomolecules responsible for the reduction of Ag^+ ion and stabilization of the Ag NPs. The observed absorption bands were compared with the standard values for the identification of the functional group (López-Moreno et al., 2016). The FTIR spectrum showed the absorption band at 3460, 2952, 2916, 2649, 1664, 1467, 1378, 1216, 1080, 832, 721, 588 cm^{-1} which indicated the presence of stabilizing agent with the nanoparticles (Fig. 1). The bands at 3460cm^{-1}; 2952, 2916 and 2649 cm^{-1}; 1664 $cm^{-1;}$ 1467 cm^{-1} corresponds the O-H stretching vibration which indicated the presence of phenol and alcohol, C-H stretching for alkanes and C-N and C-C stretching of proteins, N-H stretching indicating the presence amide linkages of the proteins respectively (Sanghdeep et al., 2016).These functional groups provide the stability to Ag NPs. The band at 1378 cm^{-1} corresponds the N=O indicating the presence of nitro compound (Lau et al., 2020). The band at 1216 cm^{-1} corresponds the C-N stretching of amines. The band at 1080 cm^{-1} indicates ethers =C-O-C symmetric stretching. The bands at 832, 721 cm^{-1} indicates C-Cl stretching of alkyl halides. The band at 588 cm^{-1} indicates C-Br stretching of alkyl halides. FTIR spectrum of dispersed Fe_3O_4 NPs in distilled water showed the absorption band at 3435, 1629, 1438, 1114, 542 cm^{-1}. The peak at 3435 cm^{-1} corresponds to the O-H stretching vibration generated from the hydroxyl group from the water on NPs (Fig. 1B). The band at 1629, 1438 and 1114 cm^{-1} was due to distilled water used for dilution. The band at 542 cm^{-1} corresponds to the stretching vibration of Fe-O bond. The shapes of the particles are nearly spherical for both the NPs (Fig. 1A, B).

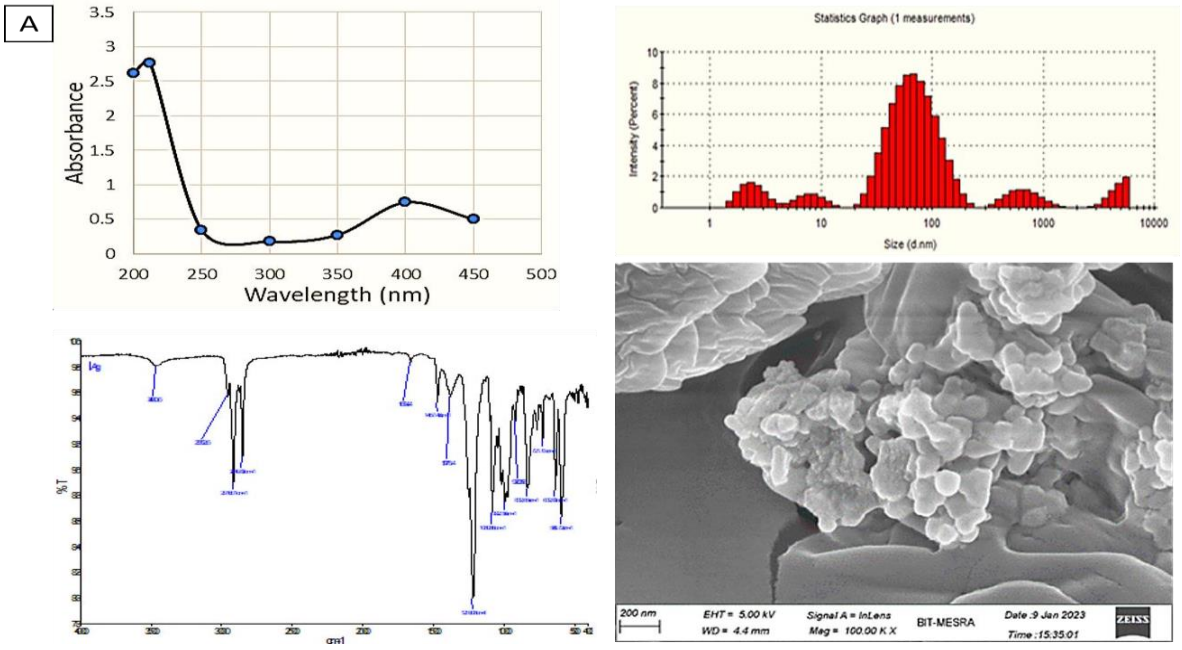

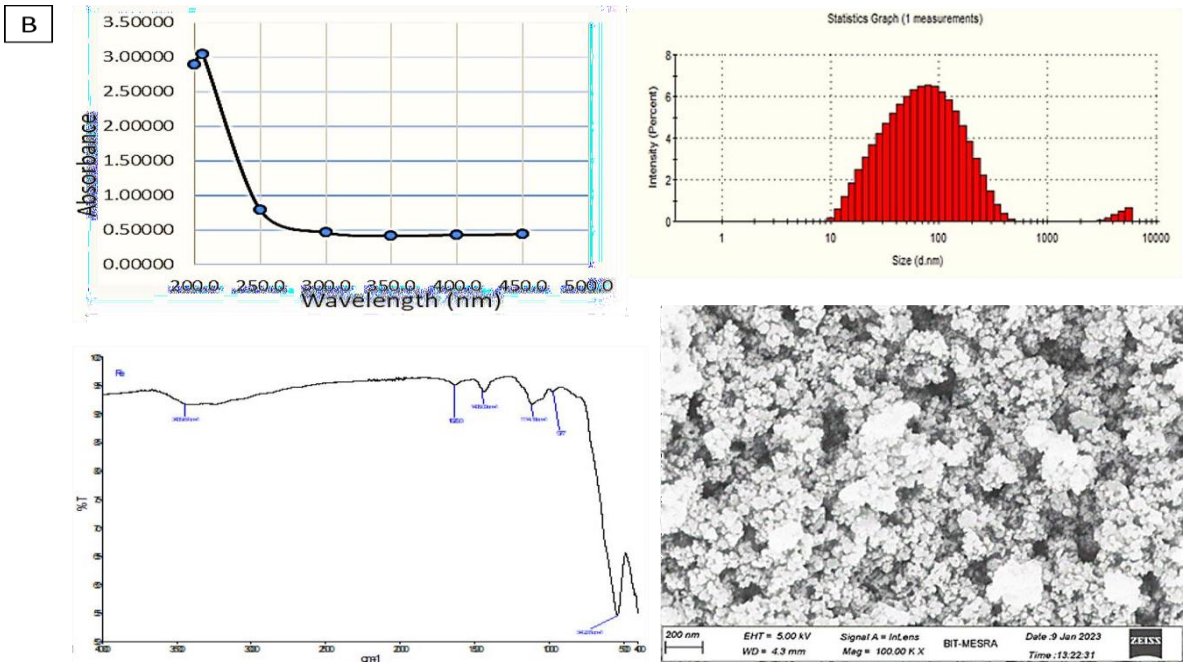

Fig. 1: Characterization results of synthesized NPs showing UV –Vis. absorbance, size scattering through DLS, functional groups analysis through FTIR, surface morphology analysis using FESEM. (A) Ag NPs (B) Fe3O4 NPs.

3.2 Morphological changes:

The morphological changes on seed germination and seedling stage after application of Ag NPs and Fe_3O_4 NP with various concentrations was observed (Fig. 2, 3).

The germination percent in *Lens culinaris* seed gradually increases from 10-40µg/mlafter the application of Fe_3O_4 NPs (56%) but in case of Ag NPs it is gradually increases from control to 30µg/ml but the value decreases in 40µg/ml from 56% to 48% (Fig. 2). In case of *M. uniflorum* seed, the germination percent gradually increases from 10-30µg/ml but similar decreasing pattern (100% to 92%) seen for 40µg/ml which may be due to toxicity effects of Fe_3O_4 NPs (Table 1A).

(A)

NPs Conc.	*L. culinaris* (Fe_3O_4 NPs)	*L. Culinaris* (Ag NPs)	*M. uniflorum* (Fe_3O_4 NPs)	*M. uniflorum* (Ag NPs)
Control	56	32	92	92
10µg/ml	45	44	96	100
20µg/ml	50	48	92	100
30µg/ml	52	56	100	100
40µg/ml	56	48	92	92

(B)

	L. culinaris (Fe_3O_4 NPs)		*L. culinaris* (Ag NPs)		*M. uniflorum* (Fe_3O_4 NPs)		*M. uniflorum* (Ag NPs)	
	Root	**Shoot**	**Root**	**Shoot**	**Root**	**Shoot**	**Root**	**Shoot**
CTR	2.8	5.06	3.3	4.7	4.36	4.66	4.36	4.83
10 µg/ml	2.7	5.39	5.86	5.26	4.83	4.46	5.15	5
20 µg/ml	3.16	4.09	3.96	5.86	4.6	5.03	6.33	5.13
30 µg/ml	4.26	3.87	3.05	3.16	5.8	5.43	6.13	4.9
40 µg/ml	3.6	2.54	2.26	4.05	4.96	4.76	5.46	4.46

Table 1: Tabular chart of germination percentage, root and shoot length of *L. culinaris*and *M. uniflorum* in different concentrations of both the NPs. (A) Germination percentage values (B) Root and shoot length of the seedlings in cm scale.

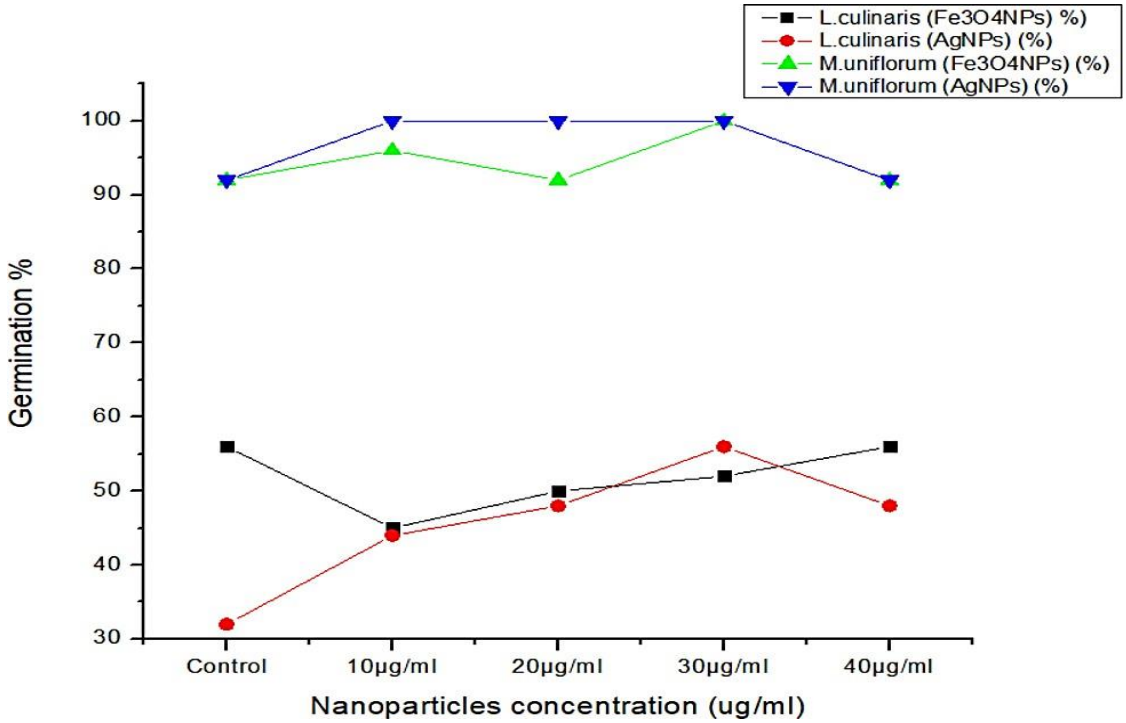

Fig. 2: Graph representation of germination percentage of both the seeds in presence of Ag NPs and Fe3O4 NPs. Black and red line represents *Lens culinaris* and blue and green colour represents *Macrotyloma uniflorum* respectively.

In case of *L. culinaris* seed root, length increases gradually from 10-30µg/ml and shoot length decreases after the application of Fe_3O_4 NPs, in case of Ag NPs root length decreases from 3.05cm to 2.26cm within the concentration range of 10-40 µg/ml and shoot length increases then it decreases (Table 1B). In case of *M. uniflorum* seed root length increased from 10-20 µg/ml, then it decreases in 30 µg/ml then it increases and shoot length increased first then it decreases after the application of Fe_3O_4 NPs, in case of Ag NPs root length increases from control to 30 µg/ml then it decreases and shoot length increases from control then it decreases in 40 µg/ml (Fig. 3).

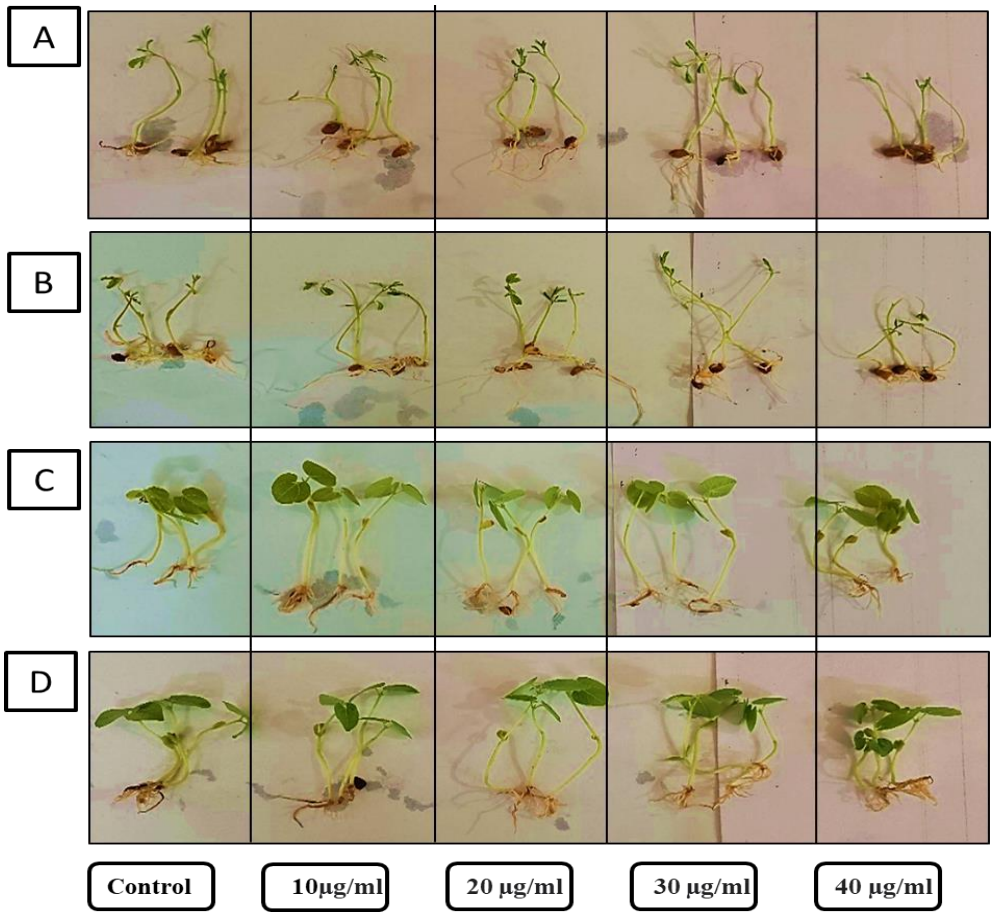

Fig. 3: Morphological alteration of root and shoot after both NPs application in four different concentrations. The first column represent control where no NPs were added. (A) L culinaris after application of Fe3O4 NPs, (B) L. culinaris after application of Ag NPs, (C) M uniflorum after application of Fe3O4 NPs, (D) M uniflorum after application of Ag NPs.

It is been reported in research article (Alkhatib et al., 2021) that more than 20 nm size of Fe_3O_4 NPs and in 30 µg/ml conc. the seedling growth rate decreased. From the seedling growth (Fig. 4 C) it was prominent that up to certain concentration (30 µg/ml) for both the NPs the seedling length (root and shoot) increased but in 40 µg/ml the percentage value dropped down. Previously in

research article of Noshad et al. (2019) it was reported about the involvement of Ag NPs in seedling growth of *Solanum lycopersicum*. Furthermore, the outcome aligns with the findings of Guzmán-Báez et al. (2021), who reported that AgNPs induced an increase in both root length and number in tomato seedlings. It can be considered that Ag NPs ability to activate cell division regulators, speed up the synthesis of photosynthetic pigment, may account for *L. culinaris* and *M. uniflorum* longer shoots and roots (Rahman et al., 2023). Furthermore, it was also noticed that *M uniflorum*have a higher shoot rate in the presence of both the NPs than the root rate, suggesting that while some seeds germinated, and the growth of the shoot was slowed down (Fig. 4 A). The experiments were performed in triplicate and proper bar graph was plotted for seed germination, root length and shoot length with NPs concentration (Fig. 4A, B, C).

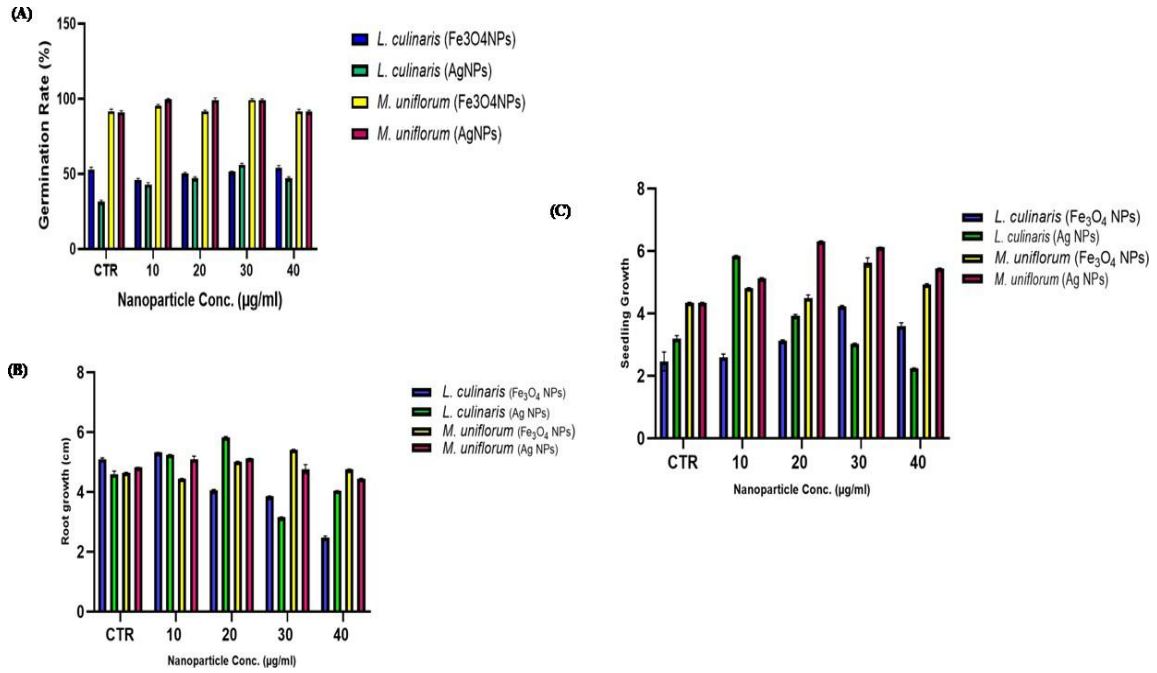

Fig. 4: Bar graph representing the effect of Ag NPs and Fe3O4 NPs on (A). Germination rate (B). Root growth (C). Seedling growth

Based on the bar graphs, it is evident that both the NPs treatments had varied effects on germination rate, root and seedling growth in *Lens culinaris* and *Macrotyloma uniflorum*.

Both the seeds showed positive response after applying NPs solution during germination stage, but *M. uniforum* showed highest germination rate at 30 µg/ml concentration for both the NPs. However, *L. culinaris* showed highest germination rate at 30 µg/ml and 40 µg/ml of Fe_3O_4 NPs and Ag NPs respectively.

The second factor observed during the experiment was root growth after germination in the seeds. *In L. culinaris* root growth was relatively stable across both the NPs concentrations, with a slight improvement for Fe_3O_4 NPs and Ag NPs up to 30 µg/ml, but showed some reduction at 40 µg/ml, particularly for Fe_3O_4 NPs. *For the other seed (M. uniflorum)*, root growth was most enhanced by Ag NPs especially at 20 and 30 µg/ml, while Fe_3O_4 NPs generally supported better root growth

at lower concentrations, showing highest peak at 20 µg/ml. The seeds of *M. uniflorum* generally responded better to Ag NPs, while *L. culinaris* showed better results with Fe_3O_4 NPs at certain concentrations. **The last parameter of morphological growth in the experiment was seedling growth**.

In case of L. culinaris, Fe_3O_4 NPs showed consistent positive effects on seedling growth, especially at 30 µg/ml. Ag NPs showed less consistent results, but also exhibited some growth enhancement at 30 µg/ml. *For the other seed, i.e M. uniflorum*, Both Fe_3O_4 and Ag NPs led to detectable increscent in seedling growth, with Ag NPs showing the most pronounced effect at 30 µg/ml. Higher concentrations of both the NPs (30 and 40 µg/ml) seem to enhance seedling growth in both species, even though root growth may decline at the highest concentration, signifying probable toxicity of NPs acting as growth inhibition at these concentrations (Fig. 5).

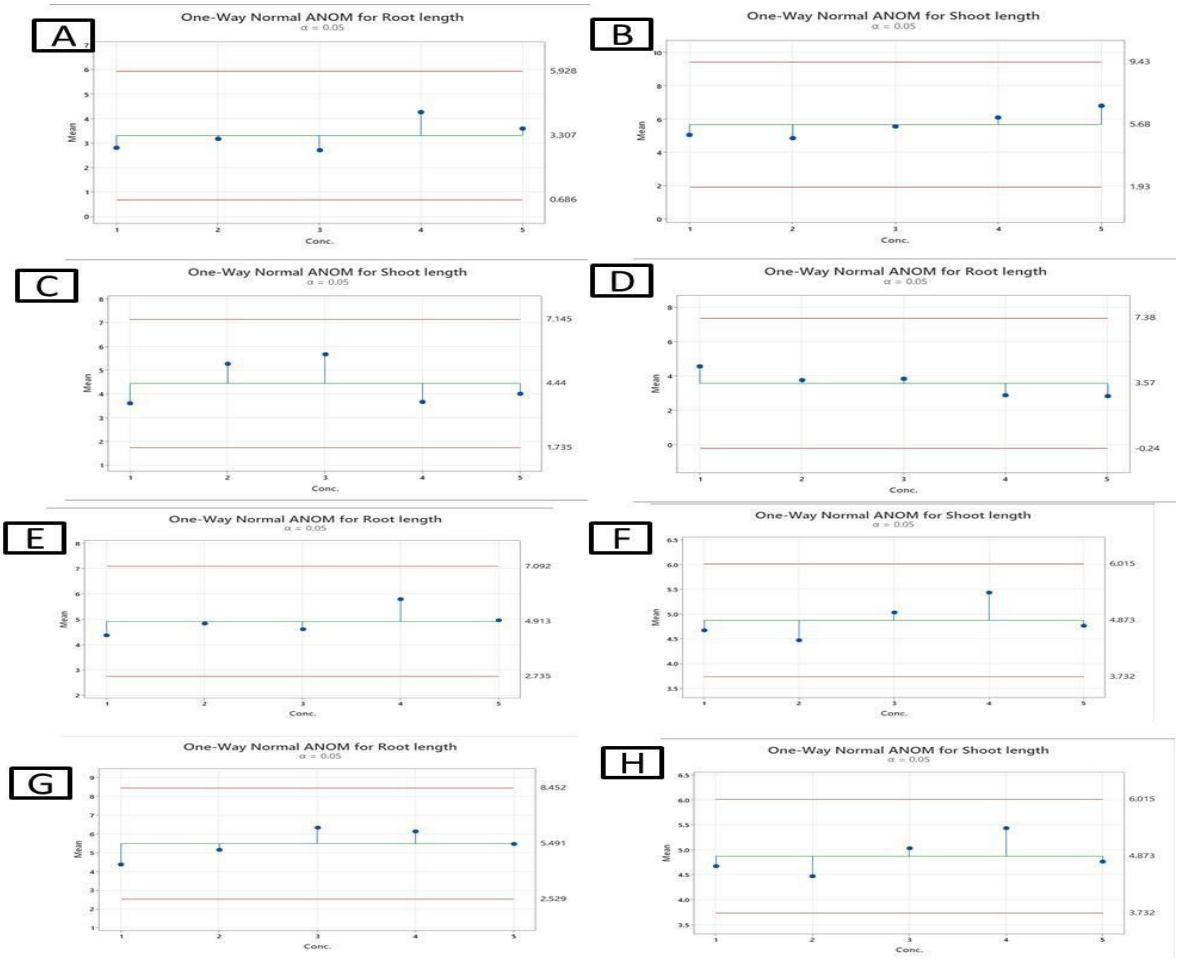

Fig. 5: Root and shoot length (A) *Lens culinaris* after application of Fe_3O_4NPs, (B) *Lens culinaris* after application of Ag NPs, (C) *Macrotyloma uniflorum* after application of Fe_3O_4 NPs, (D) *Macrotyloma uniflorum* after application of Ag NPs (the values are the mean of three replicates) 1= 0µg/ml, 2= 10 µg/ml, 3= 30 µg/ml, 4= 40 µg/ml

Total chlorophyll content in case of *Lens culinaris* seed increases from 10-40 µg/ml after application of Fe_3O_4 NPs, in case of Ag NPs it increases from control-30 µg/ml then it decreases. In case of *M.*

uniflorum seed it from control-30 µg/ml then decreases after application of Fe_3O_4 NPs, in case Ag NPs it increases from control- 10 µg/ml then it decreases (Fig. 6 A, B, C and D)

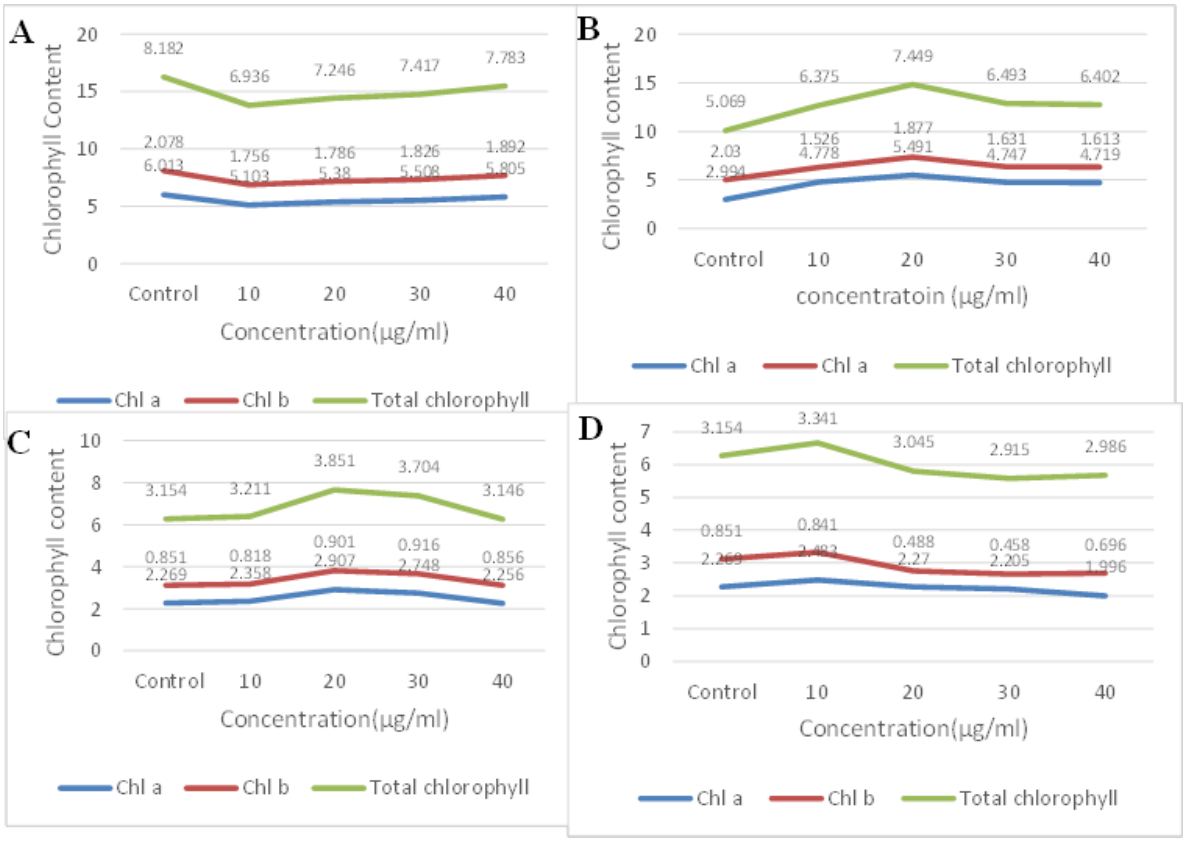

Fig. 6: Representation of chlorophyll content (A) *L. culinaris* after application of Fe_3O_4 NPs, (B) *L. culinaris* after application of Ag NPs, (C) *M. uniflorum* after application of Fe_3O_4 NPs, (D) *M. uniflorum* after application of Ag NPs

Protein estimation is done by using the Standard graph prepared earlier. From the graph (Fig. 7A) amount of proteins present in the sample can be calculated. The highest concentration of protein found in *L. culinaris* seed is in 40µg/ml (highest from all the concentration with respect to control) after the application of Fe_3O_4NPs but in case of Ag NPs it is gradually increases from 10-40µg/ml but lesser from control. In case of *M. uniflorum* seed, the protein concentration gradually increases from 10-40µg/ml but lesser from control after the application of Fe_3O_4 NPs, but after application of Ag NPs it is gradually increasing from control to 30µg/ml but lower in 40µg/ml due to toxicity of Ag NPs as shown in Fig. 7A (Sharma et al., 2021).

Overall, for the starch amount it was noticed that *M. uniflorum* seeds treated with Fe_3O_4 NPs showing very less amount (below 0.4mg) for all the four concentration of NPs (Fig. 7B). But for the starch amount found in *L. culinaris* seed gradually decreases from control to 40µg/ml after the application of Fe_3O_4 NPs. However, for Ag NPs the starch amount was not so prominent. In 20µg/ml concentration of Ag NPs the peak for starch content was highest (0.1 mg).

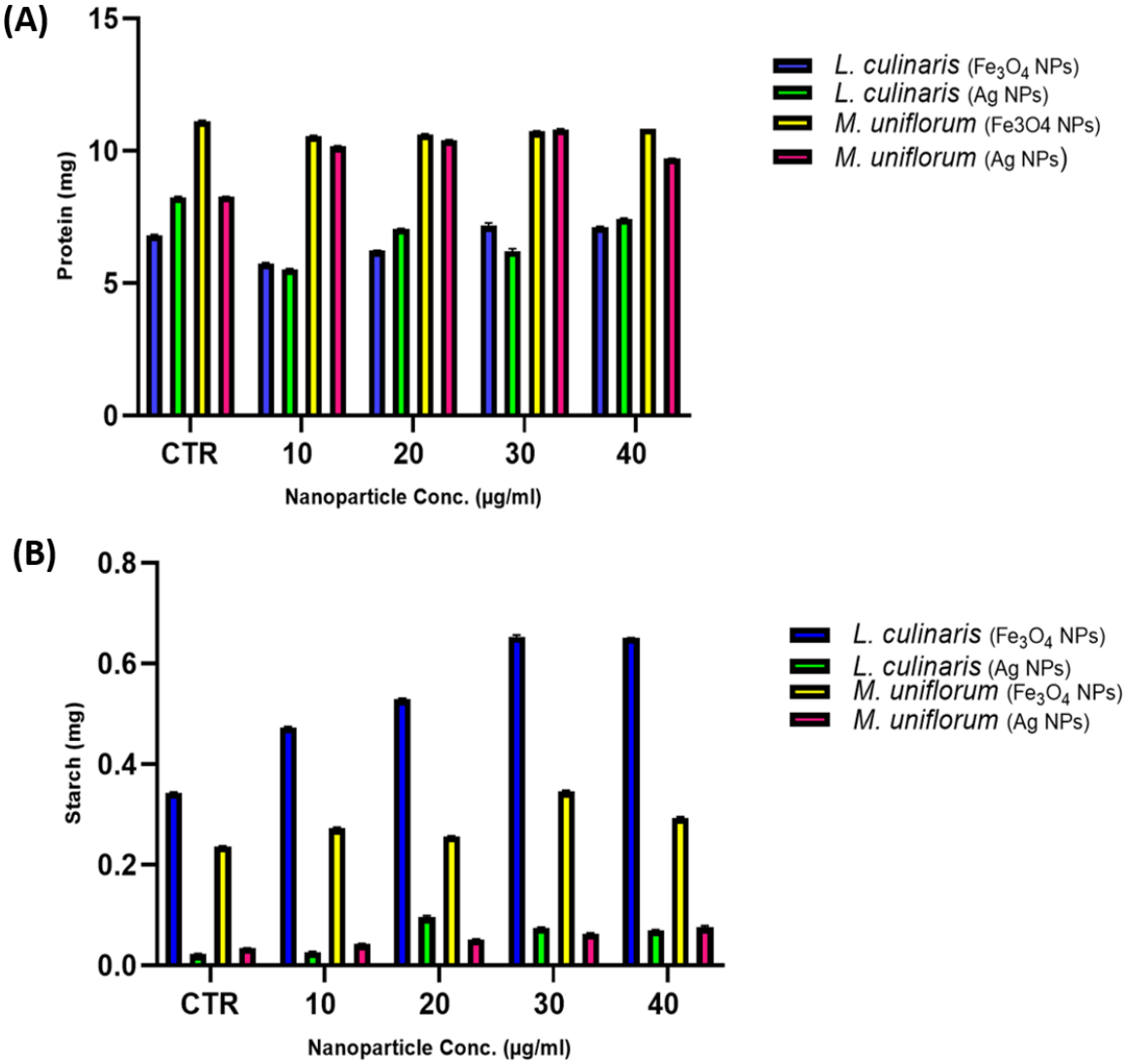

Fig. 7: Bar graph representation of protein and starch content (mg) in various concentrations of two NPs (Ag NPs and Fe3O4NPs); (A) Protein content (B) Starch content. Colour codes are provided.

3.3 ICP-OES analysis

Previous many research (Rajput et al., 2018; Patel et al., 2018) states that producing hydroxyl radicals, NP accumulation (Rajput et al., 2020) can change the physiological processes of plants and therefore can impact the integrity of the organizations at cellular and subcellular levels. That further can alter the quantity of proteins, lipids, and nucleic acids. Basically, plant roots are the main entrance and storage unit of NPs, which can then go to the shoots and other tissues of the plant, including the developing seeds (Doolette et al., 2015).This translocation of NPs is significantly influenced by both plant and NP characteristics.

In this current research, uptake and localization of synthesized Ag and Fe_3O_4 NPs was tried to be sited using visualization and analytical results. Figure 8, 9 shows LS section of both stem and root in both the seeds (*M. uniflorum* stem and *L. culinaris*) that shows localization of Fe_3O_4 NPs as black colour dot (Fig. 8A). Ag NPs shows negligible localization and was non-spotted under microscope, therefore not provided in the results of the article. From the Fig. (Fig. 9B) it is also eminent that in control condition uptake and localization not happened. Further for quantitative values of both the

nanoparticles presence in stem and root ICP-OES result is also provided in the table (Fig. 10A). For *L. culinaris,* Fe_3O_4 NPs value was highest in 30µg/ml concentration (0.657mg/ml) and Ag NPs value was drastically less (0.076 mg/ml). Overall, from the graph (Fig. 10B) it can be noticed that accumulation of Fe_3O_4 NPs is more than the Ag NPs for particularly these two seeds.

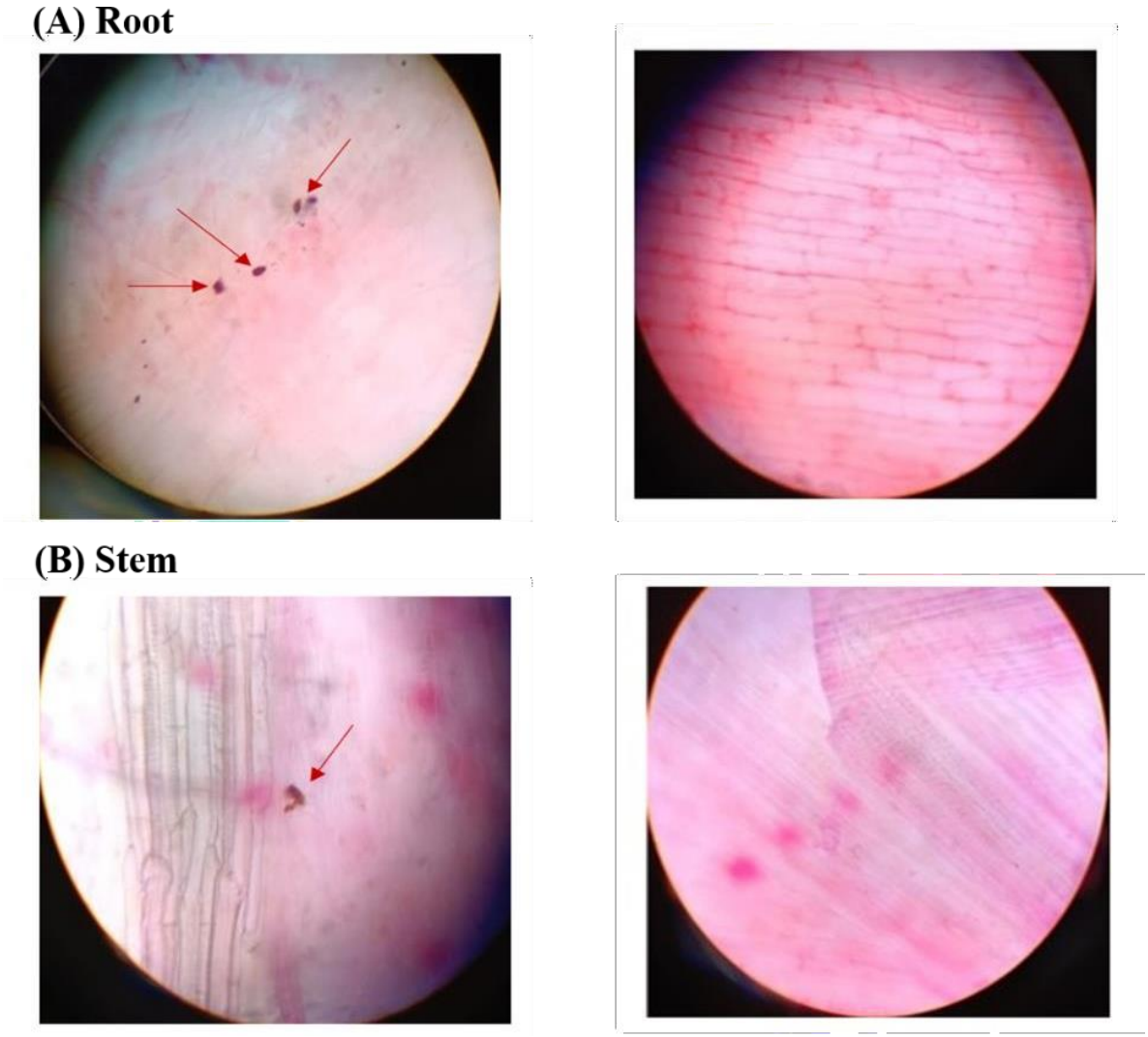

Fig. 8: Microscopic view of root and stem dissection of *M. uniflorum* in different concentrations of Fe3O4 NPs. (A) root dissection in 30µg/ml and control (B) stem dissection in 30µg/ml and control. The red coloured arrow indicates the accumulation of Fe3O4 NPs in root and stem of *M. uniflorum.*

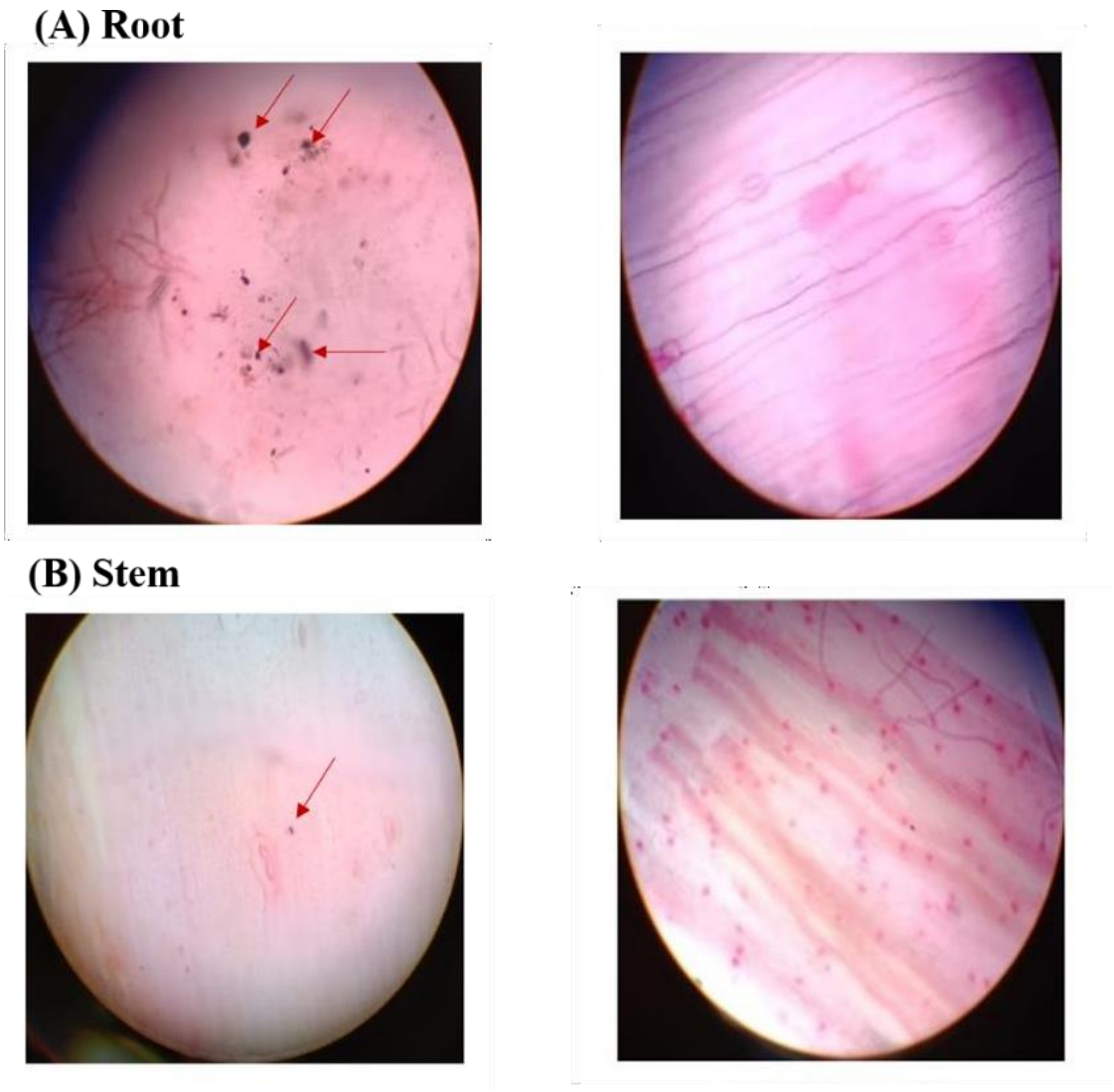

Fig. 9: Microscopic view of root and stem dissection of *L. culinaris* in different concentrations of Fe3O4 NPs. (A) root dissection in 30µg/ml and control (B) stem dissection in 30µg/ml and control. The red coloured arrow indicates the accumulation of Fe3O4 NPs in root and stem of *L. culinaris.*

(A)

Concentration in NPs (mg/ml)	*L. culinaris* (Fe_3O_4 NPs)	*L. Culinaris* (Ag NPs)	*M. uniflorum* (Fe_3O_4 NPs)	*M. Uniflorum* (Ag NPs)
Control	0.345	0.024	0.238	0.035
10µg/ml	0.479	0.028	0.275	0.041
20µg/ml	0.534	0.098	0.258	0.053
30µg/ml	0.657	0.076	0.348	0.065
40µg/ml	0.655	0.071	0.294	0.079

(B)

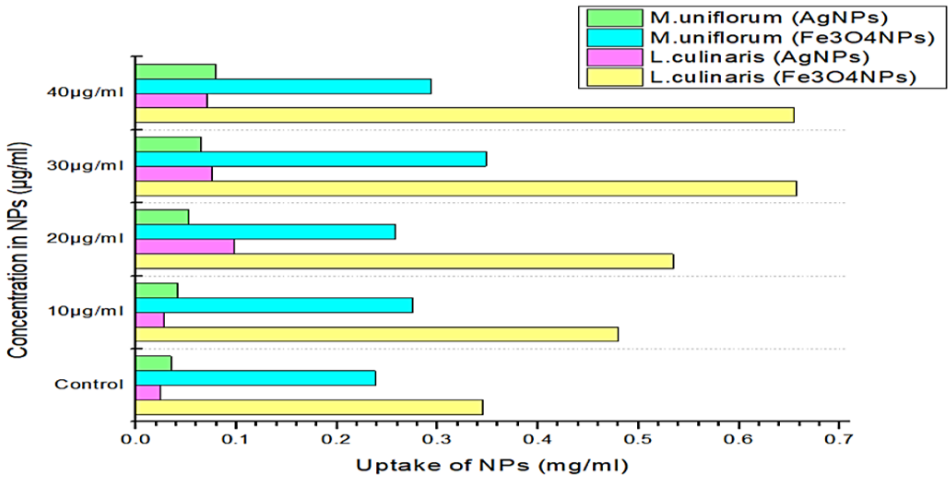

Fig. 10: Data representation of ICP-OES for Fe3O4 NPs. (A) Tabular chart showing the values for both the NPs in root and stem of *M. uniflorum* and *L. culinaris* (B) Bar graph representation of NPs uptake in root and stem

5. Conclusions

Ag and Fe_3O_4 NPs were successfully synthesized using chemical reduction and co-precipitation methods, respectively. The UV-Vis absorption spectra, DLS, FTIR, and FESEM analyses confirmed the formation, uniformity, and morphology of the synthesized NPs. The application of these NPs to *L. culinaris* and *M. uniflorum* seeds demonstrated considerable improvements in the root shoot length, germination percentage, and biochemical parameters like chlorophyll, protein, and starch content. The NP uptake analysis using the ICP-OES technique confirmed the accumulation of both the NPs within the plant tissues, mainly in roots and stems.

This experiment highlighted the potential of both these NPs as efficient growth promoters in the agricultural crops. Its proper application shows promising outcomes in germination rate and also in overall plant development. Therefore, upcoming studies should focus on the sustainable and environmental friendly synthesis approaches as well as optimize the concentrations of NPs to minimize any sort of possible damaging consequences on the crops and environment.

Author Contributions: All authors contributed to the study conception and design. Material preparation, data collection and experimental analysis have been performed by SB and NS. Manuscript editing has been done by SB and MK. The overall experiment design, monitoring and manuscript editing was performed by KM. All authors read, approved and gave consent for the final manuscript

Funding: This research has received UG-PG funds from Birla institute of technology, under B.E/M.E/M.TECH project based research grants (Ref: BT/HOD/22-23/074).

Acknowledgments: Authors are thankful to Department of Bioengineering and Biotechnology, BIT Mesra and Central instrumentation facility (CIF), BIT Mesra, Ranchi, Jharkhand, India for providing all the lab facilities and instrumentation facilities to fulfil the requirement of the experiment.

Conflicts of Interest: The authors declare no conflict of interest. The funders had no role in the design of the study; in the collection, analyses, or interpretation of data; in the writing of the manuscript, or in the decision to publish the result.

Data availability statement: The authors declare that data supporting the findings of this study are available within the article in the form of tables and figures

6. References

1. Alidoust, D. and Isoda, A., 2013. Effect of gamma Fe_2O_3 nanoparticles on photosynthetic characteristics of soybean (Glycine max (L.) Merr.): foliar spray versus soil amendment. Acta Physiologiae Plantarum, 35, pp.3365–3375.
2. Alkhatib, R., Alkhatib, B. and Abdo, N., 2021. Effect of Fe3O4 nanoparticles on seed germination in tobacco. *Environmental Science and Pollution Research*, *28*(38), pp.53568-53577.
3. Arora, S., Murmu, G., Mukherjee, K., Saha, S. and Maity, D., 2022. A comprehensive overview of nanotechnology in sustainable agriculture. *Journal of Biotechnology*, *355*, pp.21-41.
4. Avila-Quezada, G.D., Ingle, A.P., Golińska, P. and Rai, M., 2022. Strategic applications of nano-fertilizers for sustainable agriculture: benefits and bottlenecks. Nanotechnology Reviews, 11(1), pp.2123-2140.
5. Avila-Quezada, G.D., Ingle, A.P., Golińska, P. and Rai, M., 2022. Strategic applications of nano-fertilizers for sustainable agriculture: Benefits and bottlenecks. *Nanotechnology Reviews*, *11*(1), pp.2123-2140.
6. Bindraban, P.S., Dimkpa, C., Nagarajan, L., Roy, A. and Rabbinge, R., 2015. Revisiting fertilizers and fertilization strategies for improved nutrient uptake by plants. Biology and Fertility of Soils, 51, pp.897-911. doi: 10.1007/s00374-015-1039-7.
7. Bombin, S., LeFebvre, M., Sherwood, J., Xu, Y., Bao, Y. and Ramonell, K.M., 2015. Developmental and reproductive effects of iron oxide nanoparticles in Arabidopsis thaliana. *International journal of molecular sciences*, *16*(10), pp.24174-24193.
8. Chaki, S.H., Malek, T.J., Chaudhary, M.D., Tailor, J.P. and Deshpande, M.P., 2015. Magnetite Fe3O4 nanoparticles synthesis by wet chemical reduction and their characterization. *Advances in Natural Sciences: Nanoscience and Nanotechnology*, *6*(3), p.035009.
9. Chen, H.D. and Yada, R., 2011. Nanotechnologies in agriculture: new tools for sustainable development. Trends in Food Science & Technology, 22, pp.585-594. doi: 10.1016/j.tifs.2011.09.004.
10. Cheng, W., Xu, J., Wang, Y.J., Wu, F., Xu, X. and Li, J.J., 2015. Dispersion-precipitation synthesis of nanosized magnetic iron oxide for efficient removal of arsenite in water. Journal of Colloid and Interface Science, 445, pp.93-101. doi: 10.1016/j.jcis.2014.12.082.

11. Doolette, C.L., McLaughlin, M.J., Kirby, J.K. and Navarro, D.A., 2015. Bioavailability of silver and silver sulfide nanoparticles to lettuce (Lactuca sativa): Effect of agricultural amendments on plant uptake. *Journal of hazardous materials*, *300*, pp.788-795.
12. Elamawi, R.M., Al-Harbi, R.E. and Hendi, A.A., 2018. Biosynthesis and characterization of silver nanoparticles using Trichoderma longibrachiatum and their effect on phytopathogenic fungi. *Egyptian journal of biological pest control*, *28*(1), pp.1-11.
13. Guzmán-Báez, G.A., Trejo-Téllez, L.I., Ramírez-Olvera, S.M., Salinas-Ruíz, J., Bello-Bello, J.J., Alcántar-González, G., Hidalgo-Contreras, J.V. and Gómez-Merino, F.C., 2021. Silver nanoparticles increase nitrogen, phosphorus, and potassium concentrations in leaves and stimulate root length and number of roots in tomato seedlings in a hormetic manner. Dose-Response, 19.
14. Hao, Y., Zhang, Z.T., Rui, Y.K., Ren, J.Y., Hou, T.Q., Wu, S.J., Rui, M.M., Jiang, F.P. and Liu, L.M., 2016, June. Effect of different nanoparticles on seed germination and seedling growth in rice. In *2nd Annual international conference on advanced material engineering (AME 2016)* (pp. 166-173). Atlantis Press.
15. Iravani, S., Korbekandi, H., Mirmohammadi, S.V. and Zolfaghari, B., 2014. Synthesis of silver nanoparticles: chemical, physical and biological methods. *Research in pharmaceutical sciences*, *9*(6), p.385.
16. Jemal, K., Sandeep, B.V. and Pola, S., 2017. Synthesis, characterization, and evaluation of the antibacterial activity of Allophylus serratus leaf and leaf-derived callus extracts mediated silver nanoparticles. Journal of Nanomaterials.
17. Kaningini, A.G., Nelwamondo, A.M., Azizi, S., Maaza, M. and Mohale, K.C., 2022. Metal nanoparticles in agriculture: a review of possible use. *Coatings*, 12(10), p.1586.
18. Kashyap, A., Kumari, M., Kumar, S., Nazma, S., Mukherjee, K. and Maity, D., 2023. Effect of *Mangifera indica* extracted CuO NPs on Seed Germination of *Cicer Arietinum* and *Vigna Radiata*: An insight on Biochemical, Physiological and Computational Studies. *Advanced Materials Letters*, *14*(4), pp.2304-1735.
19. Kiwumulo, H.F., Muwonge, H., Ibingira, C., Lubwama, M., Kirabira, J.B. and Ssekitoleko, R.T., 2022. Green synthesis and characterization of iron-oxide nanoparticles using Moringa oleifera: a potential protocol for use in low and middle income countries. *BMC Research Notes*, *15*(1), p.149.
20. Kumari, M., Sarkar, B. and Mukherjee, K., 2023. Nanoscale calcium oxide and its biomedical applications: a comprehensive review. *Biocatalysis and Agricultural Biotechnology*, *47*, p.102506.
21. Lau, E.C., Carvalho, L.B., Pereira, A.E., Montanha, G.S., Corrêa, C.G., Carvalho, H.W., Ganin, A.Y., Fraceto, L.F. and Yiu, H.H., 2020. Localization of coated iron oxide (Fe3O4) nanoparticles on tomato seeds and their effects on growth. *ACS Applied Bio Materials*, *3*(7), pp.4109-4117.
22. López-Moreno, M.L., Avilés, L.L., Pérez, N.G., Irizarry, B.Á., Perales, O., Cedeno-Mattei, Y. and Román, F., 2016. Effect of cobalt ferrite (CoFe2O4) nanoparticles on the growth and development of Lycopersicon lycopersicum (tomato plants). *Science of the Total Environment*, *550*, pp.45-52.
23. Ma, C., White, J.C., Dhankher, O.P. and Xing, B., 2015. Metal-based nanotoxicity and detoxification pathways in higher plants. *Environmental science & technology*, *49*(12), pp.7109-7122.
24. Mahawar, H. and Prasanna, R., 2018. Prospecting the interactions of nanoparticles with beneficial microorganisms for developing green technologies for agriculture. Environmental Nanotechnology, Monitoring & Management, 10, pp.477-485.

25. Ndaba, B., Roopnarain, A., Haripriya, R.A.M.A. and Maaza, M., 2022. Biosynthesized metallic nanoparticles as fertilizers: an emerging precision agriculture strategy. Journal of Integrative Agriculture, 21(5), pp.1225-1242.
26. Noori, A., Ngo, A., Gutierrez, P., Theberge, S. and White, J.C., 2020. Silver nanoparticle detection and accumulation in tomato (Lycopersicon esculentum). *Journal of Nanoparticle Research*, *22*, pp.1-16.
27. Noshad, A., Hetherington, C. and Iqbal, M., 2019. Impact of AgNPs on seed germination and seedling growth: a focus study on its antibacterial potential against Clavibactermichiganensis subsp. michiganensis infection in Solanum lycopersicum. Journal of Nanomaterials.
28. Patel, P.R., Shaikh, S.S. and Sayyed, R.Z., 2018. Modified chrome azurol S method for detection and estimation of siderophores having affinity for metal ions other than iron. *Environmental Sustainability*, *1*(1), pp.81-87.
29. Priester, J.H., Ge, Y., Mielke, R.E., Horst, A.M., Moritz, S.C., Espinosa, K., Gelb, J., Walker, S.L., Nisbet, R.M., An, Y.J. and Schimel, J.P., 2012. Soybean susceptibility to manufactured nanomaterials with evidence for food quality and soil fertility interruption. *Proceedings of the National Academy of Sciences*, *109*(37), pp.E2451-E2456.
30. Rahman, M.S., Chakraborty, A., Kibria, A., Hossain, M.J., Noshad, A., Hetherington, C., Iqbal, M., 2023. Effects of silver nanoparticles on seed germination and growth performance of pea (Pisum sativum). Plant Nano Biology, 5, p.100042.
31. Rajput, V., Minkina, T., Fedorenko, A., Sushkova, S., Mandzhieva, S., Lysenko, V., Duplii, N., Fedorenko, G., Dvadnenko, K. and Ghazaryan, K., 2018. Toxicity of copper oxide nanoparticles on spring barley (Hordeum sativum distichum). *Science of the Total Environment*, *645*, pp.1103-1113.
32. Rajput, V., Minkina, T., Mazarji, M., Shende, S., Sushkova, S., Mandzhieva, S., Burachevskaya, M., Chaplygin, V., Singh, A. and Jatav, H., 2020. Accumulation of nanoparticles in the soil-plant systems and their effects on human health. *Annals of Agricultural Sciences*, *65*(2), pp.137-143.
33. Rashid, M.U., Bhuiyan, M.K.H. and Quayum, M.E., 2013. Synthesis of silver nano particles (Ag-NPs) and their uses for quantitative analysis of vitamin C tablets. *Dhaka University Journal of Pharmaceutical Sciences*, *12*(1), pp.29-33.
34. Rastogi, A., Zivcak, M., Sytar, O., Kalaji, H.M., He, X., Mbarki, S. and Brestic, M., 2017. Impact of metal and metal oxide nanoparticles on plant: a critical review. *Frontiers in chemistry*, *5*, p.78.
35. Rico, C.M., Lee, S.C., Rubenecia, R., Mukherjee, A., Hong, J., Peralta-Videa, J.R. and Gardea-Torresdey, J.L., 2014. Cerium oxide nanoparticles impact yield and modify nutritional parameters in wheat (Triticum aestivum L.). *Journal of agricultural and food chemistry*, *62*(40), pp.9669-9675.
36. Sanghdeep, G., Pragati, M., Shukla, P.K. and Ramteke, P.W., 2016. Effect of engineered iron-oxide and copper oxide nanoparticle on the germination and growth on soybean (Glycine max L.). *International Journal of Plant Sciences (Muzaffarnagar)*, *11*(1), pp.51-54.
37. Seleiman, M.F., Almutairi, K.F., Alotaibi, M., Shami, A., Alhammad, B.A. and Battaglia, M.L., 2020. Nano-fertilization as an emerging fertilization technique: why can modern agriculture benefit from its use? Plants, 10(1),
38. Sharma, P., Gautam, A., Kumar, V. and Guleria, P., 2021. In vitro exposure of magnesium oxide nanoparticles adversely affects the vegetative growth and biochemical parameters of black gram. *Environmental Nanotechnology, Monitoring & Management*, *16*, p.100483.
39. Singh, R.P., Handa, R. and Manchanda, G., 2021. Nanoparticles in sustainable agriculture: an emerging opportunity. Journal of Controlled Release, 329, pp.1234-1248.

40. Song, K.C., Lee, S.M., Park, T.S. and Lee, B.S., 2009. Preparation of colloidal silver nanoparticles by chemical reduction method. *Korean Journal of Chemical Engineering*, *26*, pp.153-155.
41. Tavares, P., Balbinot, F., de Oliveira, H.M., Fagundes, G.E., Venâncio, M., Ronconi, J.V.V., Merlini, A., Streck, E.L., da Silva Paula, M.M. and de Andrade, V.M., 2012. Evaluation of genotoxic effect of silver nanoparticles (Ag-Nps) in vitro and in vivo. *Journal of nanoparticle research*, *14*, pp.1-7.
42. Tripathi, D.K., Singh, S., Singh, S., Pandey, R., Singh, V.P., Sharma, N.C., Prasad, S.M., Dubey, N.K. and Chauhan, D.K., 2017. An overview on manufactured nanoparticles in plants: uptake, translocation, accumulation and phytotoxicity. *Plant physiology and biochemistry*, *110*, pp.2-12.
43. Yang, J., Cao, W. and Rui, Y., 2017. Interactions between nanoparticles and plants: phytotoxicity and defense mechanisms. *Journal of plant interactions*, *12*(1), pp.158-169.
44. Zaheer, Z., 2012. Silver nanoparticles to self-assembled films: green synthesis and characterization. *Colloids and surfaces B: Biointerfaces*, *90*, pp.48-52.

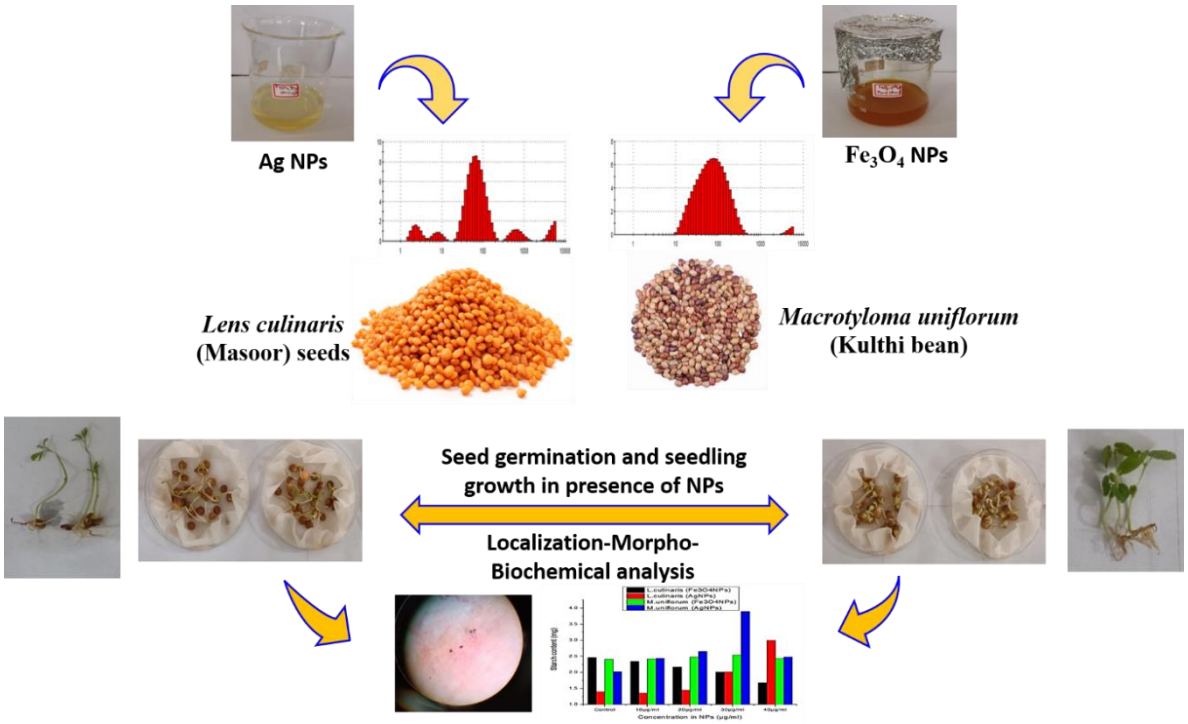

Graphical Abstract: Seed germination and seedling growth in the presence of nanoparticles can be observed along with their localization and morpho-biochemical analysis